Nanoparticles Prepared From Pterostilbene (PTE): A New Strategy for Reducing Blood Glucose and Improving Diabetic Complications

Xi Zhao
Yunnan University of Traditional Chinese Medicine
Anhua Shi
Yunnan University of Traditional Chinese Medicine
Qiong Ma
Yunnan University of Traditional Chinese Medicine
Xueyan Yan
Kunming Medical University
Ligong Bian
Kunming Medical University
Pengyue Zhang
Yunnan University of Traditional Chinese Medicine
Junzi Wu (xnfz@ynutcm.edu.cn)
Yunnan University https://orcid.org/0000-0002-2976-5299

Research

Keywords: Pterostilbene (PTE), 3-acrylamidophenylboronic acid (AAPBA), NPs (NPs), Glucose sensitivity, Drug carrier, Insulin delivery

Posted Date: April 20th, 2021

DOI: https://doi.org/10.21203/rs.3.rs-435379/v1

Abstract

Aim: New envisions are put forward on the cross application of plant extracts and biomaterials, especially new conjectures are put forward on glucose lowering nanodrug delivery systems.

Study design and methods: In this study, pterostilbene (PTE) was esterified with acryloyl chloride firstly, and then 3-acrylamidophenyl boric acid (AAPBA) and PTE esterified by acryloyl chloride were copolymerized into p(AAPBA-b-PTE). The characterization and structure of its polymer were examined. Additionally, p(AAPBA-b-PTE) nanoparticles and insulin loaded p(AAPBA-b-PTE) nanoparticles were prepared. The properties of pH, temperature and glucose sensitivity were investigated. And tested the drug loading and release of NPs. The nanoparticle toxicity was observed through cell and animal experiments, and the nanoparticle biodegradation process under physiological conditions was also observed. Finally, the effects of NPs on reducing blood sugar, antioxidation and improving micro inflammation were investigated *in vivo*.

Results: Based on PTE, we successfully synthesized p(AAPBA-b-PTE) NPs. The NPs were basically round in shape with sizes between 150 and 250 nm. It has good pH and glucose sensitivity. The entrapment efficiency (EE) of insulin loaded NPs is about 56%, and the drug loading (LC) is about 13%. The highest release of insulin was 70%, and the highest release of PTE was 85%. Meanwhile, the insulin could undergo self-regulation according to the change of glucose concentration, thus achieving an effective and sustained release. Both *in vivo and in vitro* experiments showed that the NPs were safe and nontoxic. Under physiological conditions, it can be completely degraded within 40 days. Fourteen days after the mice were injected with p(AAPBA-b-PTE) NPs, there were no obvious abnormalities in the heart, liver, spleen, lung, and kidney. Moreover, the NPs can effectively reduce blood glucose, improve the antioxidant capacity and improve the micro inflammation status in mice.

Conclusions: Using PTE as raw material, p(AAPBA-b-PTE) NPs were successfully prepared, which can effectively reduce blood glucose, improve antioxidant capacity, and reduce inflammatory response. It provided a new way for the combination of plant extracts and biomaterials to regulate and treat diseases through NPs or other dosage forms.

Background

Diabetes (diabetes mellitus, DM) is a metabolic disease characterized by high blood glucose, which is caused by defects in insulin secretion and/or insulin resistance [1]. It causes damage or appears dysfunction in various tissues, especially the eye, kidneys, heart, blood vessels, chronic nerves. Diabetic complications such as cardiovascular disease are a major cause of mortality. Glycemic instability and long-term microinflammatory state are two central factors in the development of diabetic complications [2]. At present, the most direct and effective way to treat diabetes is to supplement exogenous insulin. But daily injection of insulin reduces patient compliance and quality of life. Insufficient or excessive insulin injections, or irregular use of medications all can cause blood glucose instability [3]. Moreover, most

diabetic patients are in low antioxidant capacity and micro inflammation for a long time [4]. The decrease of antioxidant capacity refers to the decrease of superoxide dismutase (SOD) and glutathione (GSH) in the blood, while the micro-inflammatory state refers to the increase of hypersensitive C-reactive protein (Hs-CRP), interleukin-1 (IL-1), and tumor necrosis factor-α (TNF-α). The decrease or increase of these markers can predict the occurrence of cardiovascular events and the prognosis of diabetic complications. Therefore, it is necessary to improve the antioxidant capacity and long-term microinflammatory status in diabetic patients. And to find different ways to modify insulin pharmacokinetics, making its onset faster or its effect longer lasting and closer to the human pathophysiological state.

Phenylboronic acid (PBA) has always been a research hotspot in how to control blood sugar stability [5-6]. The phenylboronic acid group can be reversibly combined with sugar compounds containing cis-diol chains [7]. Under the mutual repulsion interaction of the same charge in the molecule, the polymers of the reticular carrier structure have different degrees of swelling or damage and then release the corresponding encapsulated drugs [8]. Phenylboronic acid-based nanocarriers can not only achieve effective sustained release of insulin but also can regulate their drug release rate according to the glucose concentration in the body [9]. For this reason, more and more researches are devoted to glucose-responsive drug release systems. The pH of the human physiological environment is 7.4, while the pKa range of PBA and its derivatives is generally 8.2-8.6 [10]. The pKa of glucose responsive polymer based on phenylboric acid is higher than physiological pH. Then the phenylboronic acid groups in the polymer are mostly not in the ionized state, making it difficult for the polymer to react with glucose. Therefore, the prerequisite for the application of phenylboronic acid drug carrier in the treatment of diabetes is to reduce its pKa so that it can achieve glucose-sensitive performance in a physiological environment. Researchers have tried many methods. For example, Matsumoto [11] proposed a molecular strategy to operate an insulin delivery system that is self-regulated under physiological conditions (pH7.4, 37°C). Including the use of a novel phenylboronic acid derivative {4-(1,6-dioxo-2,5-diaza-7-oxamyl) phenylboronic acid: DDOPBA}, which has a rather low pKa (∼ 7.8)，the adoption of poly(N-isopropylmethacrylamide) (PNIPMAAm) for the main chain. Zheng [12] et al also prepared an amphiphilic glycopolymer (p(LAMA-r-AAPBA)), which can be delivered through the nasal cavity with lower blood glucose. In previous studies, we used N-vinylcaprolactam (NVCL), Diethylene glycol dimethacrylate（DEGMA）, 6-O-vinylazeloyl-d-galactose(OVZG) to copolymerize with AAPBA, and successfully synthesized a variety of glucose sensitive carriers[13-15]. In summary of previous studies, whether polymers formed as thermosensitive monomers, pH sensitive monomers, polyaminoacids, glycolipid monomers, can make them glucose responsive through various process methods. But neither its degradation time nor its process has been fully elucidated, especially the functional monomer. Biomaterials can develop chronic and long-term toxicity during the *in vivo* degradation process, which may cause second damage to the human body, thus requiring further research and improvement [16].

With the continuous exploration of the development and application of traditional Chinese medicine (TCM), plant extracts in nature have gradually attracted people's attention. It has been found that many plant extracts show good effects in improving antioxidant capacity and anti-inflammatory effect. Pterostilbene (PTE), 3,5-dimethoxy-4'-hydroxystilbene, as a trans-stilbene compound, is a methylated

derivative of resveratrol. And its bioavailability is higher and more stable than resveratrol [17]. PTE has a variety of biological activities such as lowering blood lipids and blood glucose, inhibiting fungi, anti-oxidation, anti-tumor and so on [18-19]. And it also has a variety of preventive and therapeutic effects on neurological diseases, cardiovascular diseases, metabolic diseases, and blood diseases [20- 22]. The experimental study by Tastekin [23] found that the blood glucose, serum insulin and malondialdehyde (MDA) levels were close to normal after PTE administration in diabetic rats. And rats showed better morphological and structural enhancement of skeletal muscle. Kosuru [24] et al gave PTE treatment to fructose-induced diabetic rats, and found that it successfully improved blood sugar control, insulin sensitivity, reduced metabolic disorders and liver oxidative stress. PTE has obvious effects on improving the antioxidant capacity and reducing micro-inflammatory response [25]. For example, PTE can activate nuclear factor-2, which can cause high expression of heme oxygenase-1 and glutathione reductase, thus playing an anti-oxidation and anticancer role [26]. Or by activating protein kinase C reduced coenzyme Ⅱ oxidase, thereby stimulating neutrophils to produce no superoxide superoxide anion and peroxidase, which in turn decreased the expression of related inflammatory factors [27]. And these are the urgent needs of diabetic patients to improve. It is suggested that PTE can reduce blood glucose and treat diabetic complications. However, Lin [28] et al conducted pharmacokinetic studies on SD rats by intravenous injection and oral administration of PTE and found that the half-life and clearance rate of intravenous PTE was (96.6 ± 23.7) min, (37.0 ± 2.5) min, and the bioavailability of PTE by oral administration is greatly reduced. The reason may be that the first pass effect reduces the blood content of PTE. In addition, most of the plant extracts like PTE are easy to be oxidized, poor in water solubility, and low in oral bioavailability, which leads to the limitation of their wide application. Many scholars have tried to improve the bioavailability of PTE by improving the dosage form or production process. To fully exert the pharmacological activity of PTE and better act on the human diseases.

Here, we hypothesized that PTE was esterified into a high molecular material and copolymerized with AAPBA to form a glucose-responsive polymer. Then insulin was entrapped in polymers to prepare a batch of drug carriers that can release insulin intelligently. Their performance, toxicology, and therapeutics were investigated to develop a batch of safe and nontoxic glucose-responsive drug carriers. Whether it can intelligently release insulin, whether it can play the pharmacological activity of PTE, and ultimately achieve stable blood glucose, improve antioxidant capacity, and improve the micro inflammatory state, are all the focus of our research.

Materials And Methods

materials

Esterified PTE was synthesized by Hangzhou Yu Hao chemical industry; AAPBA was synthesized by Wuhan Jusheng Technology Co., Ltd.; p(AAPBA) was synthesized by ourselves; 2, 2-azobisisobutyronitrile (AIBN) was purchased from Sigma Aldrich (Shanghai, China); insulin (27 $u.mg^{-1}$) was purchased from Shanghai Macklin biochemical Technology Co., Ltd. (Shanghai, China); dimethyl sulfoxide, diethyl ether, and methanol and other analytical pure solvents were purchased from Sinopharm Chemical Reagent Co.,

Ltd. and used in storage. Human normal liver $L0_2$ cells and human hepatoma SMMC-7721 cells were purchased from Shanghai Jia yuan biological Co., Ltd. (Shanghai, China); MTT kit was purchased from Shanghai Enzyme Technology Co., Ltd. (Shanghai, China); ultrapure water was obtained from home-made in the laboratory.

Preparation of P(AAPBA-b-PTE)

Firstly, acrylic acid-PTE was prepared by using acryloyl chloride to endow the C = C double bond of pterostilbene (scheme 2A), so that it can be used as a part of polymer materials. P(AAPBA) was prepared according to our previously published protocol [13]. Next, as shown in scheme 1C, p(AAPBA-b-PTE) was synthesized via “one-pot” reported in our previous literature [14]. In the first step, a certain amount of p(AAPBA) and acrylic esterified-PTE were taken as reaction monomers (scheme 2B), and AIBN as the initiator (proportion shown in Table 1), mixed in DMF and water (DMF: water = 9:1 ml), sealed in 50 ml round bottom flask. The second step is to use a vacuum pump to pump out the air and nitrogen until the bubbles disappear, then fill the flask with enough nitrogen, repeat three cycles, and place the flask in an oil bath for 12 hours (The temperature is 70 °C and the speed is 20 r/min) (scheme 2C). Finally, the reaction flask was placed in ice water to stop the polymerization, the solution was precipitated in ether three times, filtered, and dried in a vacuum for 24 hours. Then p(AAPBA-b-PTE) was obtained.

Characterization of p(AAPBA-b-PTE)

^{1}H NMR：Weigh 5mg of the sample to be tested in a Nuclear magnetic tube, the solvent is deuterium with water + deuterium with sodium hydroxide, vortex for 1 min to mix the sample thoroughly, take 5mL into the NMR tube, test and analyze on the machine, the instrument uses Avance400 nuclear magnetic Resonance spectrometer (Japan Electronics Co., Ltd.Beijing，China), and the results were analyzed by MestReNova software.

FT-IR：Weigh 5 mg of the sample to be tested, dry it in a vacuum, and grind it into powder. The scanning method is used in infrared measurement, and the scanning range is 400-4000 cm^{-1}, and the scanning interval is 4 cm^{-1}. The FT-IR samples were collected and recorded with spectral data, and their chemical structures were deduced according to the characteristic absorption peaks. A thermal scientific nicolettis5 Fourier infrared spectrometer (Thermo Fisher Scientific, Hercules, USA) was used, and the results were analyzed by OriginPro 9.0 software.

TG and TGA：The 5 mg samples were tested in a small dry spot under the condition of nitrogen at a rate of 10^{o}C/ minutes, and the results were detected by the thermogravimetric analyzer (TGA5500, TA Instruments Co., Ltd., Newcastle, USA). The results were carried out by OriginPro 9.0 analysis software.

GPC：Weigh 5 mg of the sample, dissolve it in 25 ml of tetrahydrofuran solution and use Gel Permeation Chromatography instrument (Waters LLC, Massachusetts, USA) to detect it at a flow rate of 1.0 mL/min and a temperature of 35 °C. After the measurement, the molecular weight (Mw, Mn) and molecular weight distribution of the sample can be obtained.

DLS：The 5 mg sample was weighed and dissolved in distilled water to prepare a solution with a concentration of 1 mg/ml. The hydrodynamic diameter (Dh (Particle size)) and polydispersity index (PDI) of the NPs in water were measured by dynamic light scattering (DLS). The results were expressed as mean ± standard deviation. (n=3)

Preparation of p(AAPBA-b-PTE) NPs

Firstly, the p(AAPBA-b-PTE) of 5 mg is dissolved in a mixed solution of 2 mL DMSO and water (1:1v/v). Then slowly add it to 600 rpm's 20mL pure water and place a small magnet in it. After 3 hours of 4 ^{o}C ice water bath, the suspension was centrifuged with 12000rpm in a low-temperature high-speed centrifuge for 10 minutes. Then dispersed into ultra-pure water (10 mL), transferred to a dialysis tube (MWCO6000) for dialysis for 72 hours (room temperature), and the water was changed every 4 hours during dialysis to remove organic solvents. Then freeze it in -79 ^{o}C refrigerator for 12 hours, and finally freeze-dry it in -55 ^{o}C in a vacuum freeze-dryer to obtain p(AAPBA-b-PTE) NPs without insulin.

Properties of p(AAPBA-b-PTE) NPs

TEM：Under the condition of 38 ^{o}C, the sample suspension of 1mg/mL was added to the copper net covered with Formvar and carbon film one by one with an eyedropper. After the solvent was completely evaporated, the sample was prepared by drying. A transmission electron microscope (JEM-2100, JEOL, Japan) is used to select different areas for signal acquisition.

Zeta potential：During the determination, 0.4 mg samples were dispersed in 1 mL deionized water. It was determined by Zeta potential analyzer (Zeta PALS/90 plus, Brookhaven Instruments Corporation, New York, USA).

pH sensitivity test: The 4 mg samples were placed in phosphate-buffered saline (PBS,10 mL) with pH of 5.5, 6.0, 6.5, 7.0, 7.5, 8.0, 8.5, 9.0, 9.5 and 10.0, and the particle size distribution of the samples in the aqueous phase was measured by dynamic light scattering nanoparticle size analyzer (DLS). The instrument used in the determination is the Zeta sizer Nano S instrument (Malvern Instruments, Malvern, UK).

Temperature sensitivity test: Dissolved 4 mg NPs in 10 mL PBS aqueous solution with a pH of 7.4, and then controlled the temperature at 10, 15, 20, 25, 30, 35, 40 and 45 ℃. DLS was used to detect the change of particle size.

Glucose sensitivity test: The samples were dissolved in a 10 mL pH aqueous solution of 7.4 PBS, then the glucose concentration of PBS solution was adjusted to -0.5, 0, 0.5, 1, 1.5, 2, 2.5, 3, 3.5 g/L, and the particle size was detected by DLS.

Elastic test: The sample was taken in a 10 mL PBS aqueous solution with a pH value of 7.4, and then the glucose concentration of PBS solution was adjusted to 0, 3, 0, 3, 0, 3, 0, 3 g/L. The hydrodynamic diameter was measured by DLS.

Preparation of p(AAPBA-b-PTE) NPs containing insulin

The preparation method of insulin-encapsulated p(AAPBA-b-PTE) NPs is basically the same as that of insulin-free p(AAPBA-b-PTE) NPs. The difference is that a certain amount of insulin is weighed in advance and the p(AAPBA-b-PTE) of 50 mg is dissolved in the mixed solvent (1:1v/v) of DMSO and water of 2mL. The follow-up operation is consistent with the preparation of insulin-free NPs.

Detection of drug loading and sealing rate: After the p(AAPBA-b-PTE) NPs containing insulin were obtained, they were centrifuged with 12000 rpm and washed with water three times. The drug loading and entrapment efficiency of insulin were determined by the BCA method, and the amount of free insulin in the supernatant after BCA reaction was measured by the Bradford method and ultraviolet spectrophotometer (Shimadzu UV2550) at 562 nm. The entrapment efficiency (EE) and drug loading (LC) of NPs are calculated using the following formula:

EE= (total insulin mass-free insulin mass) / total insulin mass × 100%;

LC= (total insulin mass-free insulin mass) / mass of NPs × 100%

All measurements were repeated three times and averaged.

Insulin release test: 5mg loaded insulin p(AAPBA-b-PTE) NPs were dispersed in 20mL PBS (0.1 m) aqueous solution with a pH of 7.4 and a temperature of 37 ℃. The glucose concentration of the aqueous solution was 0,1,2 and 3 mg/mL, respectively. Under the condition of 100 rpm oscillation, the drug release was determined at a fixed time point. When sampling, the supernatant of 1mL was taken out with a liquid transfer gun, and then a fresh preheating buffer was added (without insulin). After that, the content of free insulin was detected by ultraviolet spectrophotometer and BCA reagent under 562 nm.

PTE release test: The chromatographic column was X select HSS T3 column (4.6 mm × 250 mm, 5 μm), the flow rate was 0.8 ml/min, the mobile phase was acetonitrile-water (60:40), the detection wavelength was 306 nm, and the injection volume was 10 μL. Mix 20 mg of PTE with 200 ml distilled water, disperse and dissolve with ultrasonic wave, and fix the volume of the release medium as mother liquor. Take a certain amount of mother solution into the buffer solution, and prepare six different concentrations of PTE solutions (10, 20, 30, 40, 60, 80 μ $g.ml^{-1}$) respectively. Then determine the absorbance at 306nm, and obtain the drug release curve of the carrier. The standard curve of PTE was drawn according to the relationship between concentration and absorbance, and the standard curve equation (y = 80824x + 51438, R^2 = 0.9996) was established to calculate the drug release rate.

Examination of degradation: Weigh 5 mg of p(AAPBA-b-PTE) NPs and ultrasonically disperse them in a conical flask filled with 10mL standard buffer solution (pH = 7.4), put them in a constant temperature oscillator, centrifuge one sample at regular intervals at 37 ˚C, freeze-dry to obtain residues, and use transmission electron microscope (JEM-2100, JEOL, Japan) to select different areas for signal observation of morphological characteristics.

Circular dichroism detection (CD spectrum): 5 mg insulin solid powder and insulin loaded p(AAPBA-b-PTE) NPs were measured directly using BRIGHT TIME Chirascan (Jasco-815, UK Applied Optophysics).

Cell viability

The survival rate of p(AAPBA-b-PTE) NPs was evaluated by using human normal liver $L0_2$ cells and human hepatoma SMMC-7721 cells. MTT reagent was purchased from Promega company, and the experimental method was operated according to the instructions provided by the manufacturer. SMMC-7721 cells in the logarithmic growth phase were digested and separated with 0.25% trypsin, and then resuspended in RP-mi-1640 medium containing 10% fetal bovine serum. The number of cells was adjusted to 5×10^4 cells/ml, and 200 μl per well was added to the 96 well culture plate. $L0_2$ cells were cultured in a DMEM medium. Cells containing 20% fetal bovine serum were cultured in a humid environment containing 5% CO_2 at 37 °C. Then, different concentrations of p(AAPBA-b-PTE) NPs were added to the plate for incubation. After 24 hours, 40 μl of 5 ug/ml MTT solution was added to each well, and the culture was continued at 37 ℃ for 4 hours. The supernatant culture medium in each well was sucked and discarded, and 300 μl DMSO was added into each well. The absorbance value (A) at 570 nm was detected by enzyme reader (BS-1101, Huatai hehe (Beijing) Trading Co., Ltd., China). According to the following formula: cell survival rate (%) = (average a value of experimental group/average a value of blank control group) × 100%. (n=3)

Animal toxicology study

24 Kunming mice (19-23 g, half male and half female) were randomly divided into 4 groups. All animal experiments were approved by the animal use and ethics committee of Yunnan University of Chinese Medicine. In addition, All the mice used in this experiment were purchased from the department of experimental zoology, Kunming Medical University, animal qualification No. SYXK (Dian) K2020-0006.

The mice in the experimental group were intraperitoneally injected with p(AAPBA-b-PTE)2 NPs of 10, 50 and 100 mg/kg/d, respectively. The control group was injected with normal saline of 1ml/kg/d. Two weeks later, the blood was taken from the laboratory department of the first people's Hospital of Yunnan Province to detect RBC, WBC, MCV, HCT, and other blood routine indexes by automatic biochemical instrument.

Experimental design

24 Kunming mice (19-23 g, half male and half female) were reared in the environment-controlled room (temperature:25 ± 2 ℃, humidity: 55 ± 5 %, and 12 h light-dark cycle). The hyperglycemia model was induced by high fat and high sugar diet for 2 months and intraperitoneal injection of streptozotocin (STZ) [29]. The successful standard of the model was that fasting blood glucose ≥ 11.1 mmol/L and the symptoms of polydipsia, polyuria, and polyuria were appeared [30]. After the successful establishment of the model, the mice were randomly divided into three groups: model group (n=6), insulin injection treated group (n=6), and p(AAPBA-b-PTE)2 group (n=6). In addition, 6 healthy mice were selected as a normal

group. After grouping, the corresponding treatment was given. During the treatment, p(AAPBA-b-PTE)2 group was given a single injection of p(AAPBA-b-PTE) nano-injection preparation coated with insulin (the injection volume was determined according to the simulated drug release in vitro), and the insulin-treated group was given insulin solution injection (0.16 mg/d, 1mg insulin was dissolved in sodium acetate solution of 0.05 mL). The model group and normal group were given normal saline injection (0.05 ml/d). The general condition and subcutaneous injection were observed daily. The blood of mice in each group at corresponding time points was collected from the tail vein, and the glucose level was determined using a glucometer (GT-1640; Guilin Renke Medical Technology Development Co., Ltd, Guilin, China). Two weeks later, all mice were anesthetized with chloral hydrate and killed. The skin and main organs (heart, liver, spleen, lung, and kidney) were collected and the staining was used to evaluate the morphology. The activity of MDA, T-AOC, GSH, and SOD in serum was detected by commercial reagent box (Nanjing Institute of construction Biology Engineering), and the expression characteristics of Hs-CRP, IL-1, IL-6, IL-8, and TNF-a were detected by ELISA Kit (Wuhan doctoral Biotechnology).

Statistical analysis

The measurement data were expressed as mean ± SD. SPSS 23.0 software was used for statistical analysis. One-way ANOVA was used to compare the mean between groups, and LSD was used to compare the mean between groups. The difference was statistically significant ($P < 0.05$).

Results And Discussion

Characterization of p(AAPBA-b-PTE)

In our study, the structure of polymer p(AAPBA-b-PTE) was analyzed by ^{1}H nuclear magnetic resonance spectroscopy and Fourier transform infrared transmission spectroscopy (FT-IR). In figures 1 and 2, we detected the ^{1}H NMR spectra of AAPBA, PTE, p(AAPBA), and p(AAPBA-b-PTE)2 and their infrared peaks, which clearly indicated that the polymerization took place successfully.

The ^{1}H-NMR spectrum of Fig.1(a) can see the individual peaks and peak positions. The spectrum of AAPBA (DMSO-d6) δ: 5.71 (2H,1-H), 6.48 (1H,2-H), 6.35 (1H,3-H), 10.0 (2H,4-H), 7.2-8.0 (the H of benzene ring). PTE shows the following assignments: 1H NMR (DMSO-d6): δ: 6.03-6.08 (2H, 1-H), 6.26 (1H,2-H), 3.73 (6H,4-H), 6.82 (1H, 5-H), 7.28-7.69 (the H of benzene ring). p(AAPBA) (NaOD + D2O; pH = 9.5) δ: 8.3 (2H-4-H), 2.23 (1H,5-H), 2.64 (2H,6-H), 2.85 (1H,7-H), 6.68-7.8 (the H of benzene ring). And the p(AAPBA-b-PTE) (NaOD + D2O; pH = 9.5) δ: 4.75(1H,1-H), 2.64 (1H,2-H), 3.67 (6H,6-H), 2.35 (4H,7-H), 8.4 (2H,8-H), 6.32-7.439 (the H of benzene ring). The trend of our results is basically consistent with the research of Zhang and Liu [31-32]. The results indicated that PTE and AAPBA were successfully polymerized.

The results of FT-IR are shown in Fig.1(b). Firstly, AAPBA has four main characteristic absorption bands, which are C = O str (1660 cm^{-1}), C = C str (1640 cm^{-1}), o-b-o (1351 cm^{-1}). Moreover, we can see that the benzene ring skeleton of AAPBA exists between 1555cm^{-1} and 1610cm^{-1}, and there is an absorption peak

of m-substituted benzene at 698 cm-1. There are two main characteristic peaks of PTE, C = C str (1660 cm^{-1}), CH_3 str (1370 cm^{-1}) and C = O str (1510 cm^{-1}). In p(AAPBA-b-PTE)2, we can see that the absorption peaks of C = C of PTE and AAPBA have disappeared, which proves that the polymerization is successful. And the FT-IR spectra of p(AAPBA-b-PTE)2 showed two obvious absorption peaks of PTE (1370 cm^{-1}, 1510 cm^{-1}), which proved that PTE was successfully embedded in p(AAPBA-b-PTE) polymer. Compared with p(AAPBA), p(AAPBA-b-PTE)2 has an o-b-o STR absorption peak at 1330 cm^{-1} and an NH absorption peak at 1560 cm^{-1}, which indirectly proves that AAPBA has been successfully incorporated into the polymer. Curcumin similar to PTE also has anti-inflammatory, anti-cancer, anti-virus, and other pharmacological activities, but also shows poor solubility and bioavailability [33]. To date, several curcumin carriers have been synthesized as drug delivery systems using viruses, liposomes, magnetic NPs (NPS), ultrasound microbubbles, and so on [34-35]. Meng [36] successfully prepared zein/carboxymethyl dextrin NPs to encapsulate curcumin. There may be electrostatic interaction and hydrogen bonding between zein and CMD in the formation of composite NPs. The characteristic peaks of curcumin disappeared or transferred in zein/CMD-cur NPs. Our results are similar. The little characteristic peaks of the PTE have disappeared or shifted, which confirmed that we have successfully prepared PTE as part of the NPs.

Fig. 1(c) shows the thermogravimetric (TG) curves of p(AAPBA-b-PTE)1 and p(AAPBA-b-PTE)2 and the derivative thermogravimetric (DTG) curves of p(AAPBA) and p(AAPBA-b-PTE)2. TG results show that the higher the temperature, the lower the weight of p(AAPBA-b-PTE). The TG curves decrease sharply between 100 ℃ and 350 ℃, indicating the removal of solvent molecules from the sample. DTG results mainly showed three degradation temperatures of p(AAPBA-b-PTE)2. It was 290 ℃, 342 ℃, and 404 ℃. And it can be seen that there are two degradation stages at about 342 °C and 407 °C for p(AAPBA). The first degradation temperature of p(AAPBA-b-PTE)2 can be considered as hydrogen-bonded free group. The second degradation temperature of p(AAPBA) and p(AAPBA-b-PTE)2 is 342 ℃, which may be the thermal decomposition temperature of the side chain residues. The peaks of p(AAPBA) at 407 ℃ and p(AAPBA-b-PTE)2 at 404 ℃ are the thermal degradation temperature of the main chain. These results demonstrated that p(AAPBA-b-PTE) was stable and thermolytic. The molecular weight and polydispersity index (PDI) of p(AAPBA-b-PTE) are shown in Table S1. With the decrease of PTE content in p(AAPBA-b-PTE), its MW, Mn gradually increased. And the PDI was stable.

Performance of p(AAPBA-b-PTE) NPs

Since the pKa of PBA and its derivatives is much higher than the pH of the human body, it does not have ideal glucose sensitivity in pH 7.5 [37]. To ensure that glucose sensitivity can be maintained under physiological conditions, the copolymers need to reduce pKa (pH in the human body to maintain dynamic balance). Therefore, we measured the pH, temperature and glucose sensitivity of p(AAPBA-b-PTE) NPs, and comprehensively considered its performance in human physiological environment.

Fig.2(a) shows the results of pH, temperature, and glucose sensitivity of p(AAPBA-b-PTE) NPs. Firstly, the size of p(AAPBA-b-PTE) NPs increases with the increase of pH, which may be related to the pH sensitivity of AAPBA. When the pH is between 6.0 and 6.5, the particle sizes of NPs are in a relatively stable state. When the pH is greater than 6.5, phenylboronic acid groups begin to appear in AAPBA, which induces the increase of the size of NPs. It has good glucose sensitivity under physiological conditions. Secondly, the particle size of p(AAPBA-b-PTE) NPs was stable at 12.5-17.5 ° C. The higher the temperature, the larger the particle size. Finally, p(AAPBA-b-PTE) NPs have good glucose sensitivity.

When the glucose concentration was 1.5 g/L (the general blood glucose value of diabetic patients), p(AAPBA-b-PTE) NPs began to show good glucose sensitivity. It is suggested that the p(AAPBA-b-PTE) NPs can intelligently release insulin in diabetic patients. Compared with our previously prepared p(NVCL-co-AAPBA) NPs [13], the addition of PTE did not damage the phenylboronic acid functional group, which had a more stable glucose sensitivity. The results of structural stability test of p(AAPBA-b-PTE) NPs shows that the particle size was relatively stable within 35 days of storage, and there was little difference in particle size. It has been reported that the particle size of NPs can affect drug release, cell uptake, and so on, which is an important parameter to determine the drug delivery efficiency of NPs [38]. If the prepared NPs can intelligently adjust the particle size under human physiological conditions, it is easier to disperse in various parts of the body through the barrier. In terms of our results, the particle size distribution and the law of change are beneficial to use in the treatment of diabetes.

It is a challenge to achieve reversible and repeatable release of glucose-sensitive drugs under physiological conditions. Fig.2(b) shows that p(AAPBA-b-PTE) NPs have good dynamic regulation properties and reversible glucose sensitivity. When p(AAPBA-b-PTE) NPs were treated with 3 g/L concentration of glucose, they swelled and the particle size gradually increased. Then it was placed in 0 g/L glucose concentration, and its size was significantly reduced, close to the original size. Repeated, the results are consistent. This suggests that the prepared NPs can adapt to different concentrations of blood glucose by improving the particle size. The trend of the results is consistent with the characteristics of NPs prepared by Wu [14]. In the presence of glucose, more phenylboronic acid groups are transformed from hydrophobic Nonionic groups to hydrophilic, negatively charged phenyl borate esters, so the swelling degree of NPs increases. The introduction of phenylboronic acid groups made the p(AAPBA-b-PTE) NPs exhibit an obvious glucose response.

Next, we observed the size of p(AAPBA-b-PTE) NPs by DLS and analyzed its stability by Zeta potential. The results are shown in Fig.3(c). The size of NPs is about 170 nm and the zeta potential is negative. The circulation of the nano-drug delivery system with negative charge on the surface will be longer in the blood. With the decrease of PTE content in p(AAPBA-b-PTE) NPs, the zeta potential becomes larger and larger, and its absolute value becomes smaller and smaller. The lower the absolute value of zeta potential is, the more likely it is to condense. This indicated that the PTE made p(AAPBA-b-PTE) NPs more stable and dispersed. Also, the distribution of PDI did not change significantly. It is confirmed that p(AAPBA-b-PTE) NPs are uniformly distributed and exhibit good dispersion stability.

Fig. 2(d) is the TEM diagram of the p(AAPBA-b-PTE) NPs. It can be seen that NPs are spherical, but there is aggregation adhesion. Compared with that in PBS solution, the NPs containing insulin appeared large pieces of fusion in glucose solution, the particle size was obviously enlarged, and the distribution was also gradually broadened. This indicated that the NPs containing insulin could effectively decompose and release insulin in glucose solution. Guo [39] et al synthesized an amphiphilic block sugar copolymer (P(AAPBA-b-GAMA) from phenylboronic acid and carbohydrates. It was spherical with good dispersibility. Ayubi [40] et al modified the surface of magnetic NPs□MNP@PEG-Cur□with pegylated curcumin, the NPs showed aggregation and adhesion. The p(AAPBA-b-PTE) NPs also has adhesion and poor dispersion. It may be that the esterified PTE combined with AAPBA is easier to swell and aggregate in glucose solution.

With the great interest of researchers in the drug product development of NPs, more methods are needed to evaluate the quality, safety, and efficacy of NPs. Li [41] summarized the pharmacokinetic modeling and simulation methods based on physiology to describe and predict the absorption, distribution, metabolism, and excretion of NPs *in vivo*. The degradation process of p(AAPBA-b-PTE) NPs was observed by TEM. Fig.S2 shows that p(AAPBA-b-PTE) NPs are completely degraded within 40 days. Firstly, the NPs began to swell in one day and spread out. After 3 days, the reticular structure was seen and diluted. After10 days, only a few NPs have not been degraded, and the rest have been dissolved. After 40 days, the NPs were observed to be substantially degraded completely under a 500 nm microscope. The results also indirectly confirmed that the p(AAPBA-b-PTE) NPs could be effectively degraded under the human physiological environment. Zhang [42] et al prepared a multifunctional microgel by precipitation emulsion method with N-isopropyl acrylamide (NIPAAm), ethyl methacrylate (2-dimethylamino) methacrylate (DMAEMA), and AAPBA, and they would degrade gradually with time (the specific degradation complete time has not been indicated). In the physiological environment of human body, PTE releases its own pharmacological activity, which makes the structure of p(AAPBA-b-PTE) NPs dissolve and then be absorbed in the body.

Insulin loading and release of PTE

According to the performance test results of p(AAPBA-b-PTE) NPs, we tried to encapsulate insulin in NPs and intelligently release in diabetic patients. The results in Table 2 shows that the EE of insulin loaded p(AAPBA-b-PTE) NPs is about 56%, and the LC is about 13%. Moreover, it can be seen that the EE and LC fluctuate little and are stable. However, the EE of insulin NPs prepared by MumuniMA [43] et al with chitosan and water-soluble snail mucin is 88.6%. Chen [44] prepared spherical NPs from six-armed star-shaped poly(lactide-co-glycolide)(6-s-PLGA) NPs that were used to encapsulate puerarin (PU-NPs). Its EE had 89.52 ± 1.74% and LC had 42.97 ± 1.58%. It is speculated that the reason for the relatively low EE of p(AAPBA-b-PTE) NPs is that insulin is a hydrophilic drug, which is easy to enter the outer water phase from the organic phase. But overall, PTE formed a more compact complex structure with AAPBA. Fig.3(a) shows the insulin release characteristics of p(AAPBA-b-PTE) NPs. Next, the release rule of insulin from p(AAPBA-b-PTE) NPs was analyzed. As can be seen from Fig. 3(a), at 1 ml and 3 ml glucose concentrations, insulin got a rapid release within 10 h and remained stable after 30 h with the release

amount up to 70%. And the insulin release of p(AAPBA-b-PTE)2 increased with the increase of glucose concentration. The release trend of p(AAPBA-b-PTE)2 is similar to that of p(AAPBA-b-PTE)1, and it has a suitable release amount. From the point of view of saving environmental protection and performance, we consider choosing p(AAPBA-b-PTE)2 for related research. Meanwhile, the CD spectra results (Fig.S2) concluded that the structure of insulin in NPs was not destroyed. The CD spectrum of insulin released from NPs was basically consistent with that of standard insulin. Insulin could be effectively encapsulated in p(AAPBA-b-PTE) NPs. This also indirectly illustrated that the hypoglycemic effect of insulin was not impaired because it was encapsulated in the NPs.

PTE, as a plant extract, has the effect of reducing blood glucose and treating diabetic complications. The pharmacokinetics of PTE has been fully confirmed in animal and human [45]. We examined the pharmacological activity and release pattern of PTE from p(AAPBA-b-PTE) NPs under glucose concentration. Fig.3(b) results shows that p(AAPBA-b-PTE) NPs could effectively release PTE. The release amount of PTE maintained over 70% after 10 days and tended to be stable. This indicated that most of the pharmacological activity of PTE is present in p(AAPBA-b-PTE) NPs. PTE has been released efficiently and persistently in p(AAPBA-b-PTE) NPs, suggesting that we may have a superior role in the prevention and treatment of diabetic complications in animal experiments. Sanna [46] et al developed a novel cationic chitosan (CS) - and anionic alginate (ALG) - coated poly (D, l-lactide-glycolide) NPs loaded with bioactive polyphenol trans - (E) - resveratrol (RSV). PTE, a derivative of RSV, also a polyphenolic compound, has similar biological activities. The NPs encapsulated with RSV exhibited the first burst release of RSV (about 70%) within 30 min, followed by a slow-release within 6 h. Although the first burst release of p(AAPBA-b-PTE) NPs was within 10 days, we achieved a long-lasting and effective release within 40 days, which has long-term therapeutic effects on diabetes.

After that, we used the software Origin for Ritger-Peppas to quickly fit the curve of drug release law of carrier drug delivery system. It can be seen in Table S2 that p(AAPBA-b- PTE)2 had N values ranging from 1 to 5 and R2 values higher than 0.9 at glucose concentrations of 0,1, and 3mg/ml. And k is greater than 0.89, and the transmission mechanism is NonFickian diffusion. This means that the drug release mechanism is skeleton dissolution, and the drug release is relatively complete, which can be widely used in polymer drug release system.

Toxicological research

The process of treating diabetes is long, so the drug carrier used for treating diabetes must be safe, non-toxic, and biodegradable, and will not cause secondary damage to the human body [47]. So we continued to explore the toxic and side effects of p(AAPBA-b-PTE) NPs, and compared the differences between NPs prepared at different ratios. Firstly, we evaluated through cell experiments. Cell culture is sensitive to environmental changes and can sensitively detect the existence of potentially toxic substances. We

selected human normal liver $L0_2$ cells and human tumor SMMC-7721 cells for comparison. Non-pretreated cells were used as a negative control group. They were all exposed to suspensions with different concentrations (25-125ug/mL). The results of Fig.4(a) show that the cell viability of human normal liver $L0_2$ cells is maintained above 100% after being treated with different concentrations of suspensions and different NPs. The existence of p(AAPBA-b-PTE) NPs will not damage the survival rate of human normal liver $L0_2$ cells. However, the cell viability of human liver cancer SMMC-7721 cells decreased to varying degrees after being treated with NPs and the lowest was 30%. The more PTE content in p(AAPBA-b-PTE) NPs, the higher the cell survival rate. The pharmacological activity of PTE reduces the toxicity of biomaterials, thus reducing the lethality of cells. Zhou [48] et al prepared NPs (GLPNPS) by boiling purified licorice proteins in an aqueous solution. They employed $L0_2$, MDCK, HepG2, and Caco-2 cell lines, respectively, for cytotoxicity evaluation. However, self-assembly into nanostructures did not significantly alter the cytotoxicity of GLP proteins. Compared with the p(AAPBA-b-OVZG) NPs prepared before (with low toxicity) [14], the toxicity study of p(AAPBA-b-PTE) NPs made a breakthrough. Table 5 shows that the p(AAPBA-b-PTE) NPs did not greatly affect the blood biochemical indexes of mice compared with the normal group. Lin [49] et al observed the subacute effects of low-dose combined poisoning with silica NPs (SiNPs) and lead acetate (PB) on the cardiovascular system of SD rats through blood routine and blood biochemical analysis. It was also indirectly demonstrated that p(AAPBA-b-PTE) NPs were safe and nontoxic and suitable for long-term prevention and treatment of diabetes.

The results of mouse histomorphology also confirmed the safety of NPs. It can be seen from Fig.4(b) that compared with the control group, the fat vacuoles in the liver of the diabetic group increased, the liver was damaged to some extent, and the rest tissues were almost unchanged. The mechanism of diabetes is mostly related to heredity and abnormal glucose and lipid metabolism, which are also the causes of liver damage [50]. Compared with the control group, there is no significant difference in heart, liver, spleen, lung, and kidney in the group injected with p(AAPBA-b-PTE)2 NPs, which proves once again that the NPs are safe and harmless. Compared with the diabetic group, the damage of tissues and organs is relatively reduced, and it is protected from hyperglycemia to some extent. In a chronic exposure environment, only a limited number of studies focus on evaluating the effects of inorganic NPs on organ toxicity, inflammation, immunotoxicity, and genotoxicity [51]. At present, the long-term toxicity of NPs remains to be verified [52]. But as far as our results are concerned, PTE makes the toxicity of NPs develop in a good trend.

It is worth noting that there are obvious bleeding spots after subcutaneous injection of NPs in mice. The skin tissue layer of the p(AAPBA-b-PTE)2 NPs group was clear, with orderly arrangement of epidermal cells and no obvious degeneration or necrosis of epidermal cells. However, a small amount of vasodilation and congestion, interstitial edema, inflammatory cell infiltration can be seen in the dermis; hair follicle structure, sebaceous glands and other skin appendages are normal. The current major challenge of oral insulin remains to overcome the multiple barriers of the gastrointestinal tract. Different insulin polysaccharide NPs were used to protect insulin from being chemically and enzymatically degraded in the stomach and small intestine, promote mucus permeation and finally achieve sustained

hypoglycemic effects [53]. So NPs encapsulated with insulin usually get into the body through intravenous injection. But we selected subcutaneous injection to observe the mice skin pathology. It may be that the size of NPs is relatively large, so there are some bleeding points. NPs are difficult to be absorbed subcutaneously, and capillaries have certain resistance to NPs. In the next work, we consider further improving the preparation method of NPs to make it closer to the human body barrier and achieve sustained and effective release.

Evaluation of hypoglycemic characteristics, oxidation and microinflammation *in vivo*

Under the condition of confirming that the p(AAPBA-b-PTE) NPs are safe and harmless, we further discuss the hypoglycemic effect of insulin-loaded NPs *in vivo*. Our blood glucose curves can be seen that both the control group and diabetic group remained within a stable curve range throughout the experiment. P(AAPBA-b-PTE)2 group and insulin injection treated group have an obvious hypoglycemic effect. However, their tendency to lower blood glucose was different. It can be seen from Fig. 5(a) that the blood glucose in the insulin injection treated group can be stabilized at 5-6 mmol/L within 4 hours, but then it shows a straight upward trend, and it tends to be stable after 8 hours. While in the p(AAPBA-b-PTE)2 group, the blood glucose could be kept at 5-6 mmol/L within 16 hours. P(AAPBA-b-PTE) 2 NPs have been proved to have a hypoglycemic effect *in vivo*, and can stably reduce blood sugar within 16 hours. Taili [54] synthesized carbon-NPs (CNPs) via the hydrothermal treatment of polysaccharides obtained from Arctium lappa L. They investigated the hypoglycemic effect of CNPs on a high-fat diet plus streptozotocin-induced diabetic mice. The results showed that CNPs reduced fasting blood glucose in mice after 42 days. Relatively speaking, the NPs constructed based on AAPBA have a remarkable and rapid effect of reducing blood glucose. Furthermore, due to the addition of PTE, the hypoglycemic effect is more obvious and lasting.

SOD is a kind of superoxide dismutase, which directly reflects the anti-oxidation level of the body. MDA is also a sign of oxidative stress and the final product of lipid peroxidation [55]. From Figure 5(b), we found that p(AAPBA-b-PTE)2 NPs containing insulin can up-regulate SOD activity and decrease MDA levels in diabetic mice. Compared with insulin injection group, GSH of p(AAPBA-b-PTE)2 NPs group was significantly increased ($P < 0.05$). P(AAPBA-b-PTE)2 NPs containing insulin improved the antioxidant capacity and micro inflammation status of diabetic mice by releasing the pharmacological activity of PTE. It indirectly proved that the plant extracts still had pharmacological effect in polymer sustained-release materials.

Insulin resistance is the main pathophysiological feature of diabetes. And inflammation plays an important role in the occurrence and development of insulin resistance through various cytokines and molecular pathways. It has been reported [56] that the increase of inflammatory cytokines such as TNF-α and IL-6 is related to the severity of diabetes. Hs-CRP is not only a non-specific marker of inflammation but also directly involved in cardiovascular diseases such as inflammation and atherosclerosis, which is the most powerful predictor and risk factor of cardiovascular diseases [57]. Fig. 5(c) shows that the levels

of IL-6 and TNF - α in mice treated with p(AAPBA-b-PTE)2 NPs containing insulin for 2 weeks were significantly lower than those in model group ($P < 0.05$). There is no significant difference in CRP level, but there is a downward trend. Our results suggest that p(AAPBA-b-PTE)2 NPs can reduce the levels of TNFα, IL-6, and Hs-CRP in diabetic rats and improve the inflammatory status. Pure use of biomaterials without plant extracts, such as zhang [58] prepared a multifunctional microgel from N-isopropyl acrylamide (NIPAAm), 2-dimethylaminoethyl methacrylate (DMAEMA), and AAPBA by precipitation emulsion method, which can reduce blood glucose, but has no therapeutic effect in treating diabetic complications. The cross combination of biochemical means with plant extracts broadens a new field.

Conclusions

In this study, PTE was used as part of a polymeric material to prepare NPs, reducing the toxicity of AAPBA biomaterials while also improving the poor water solubility and low bioavailability of PTE. PTE has higher stability and more sustained release characteristics in NPs. Moreover, the p(AAPBA-b-PTE) NPs fully exerted the pharmacological activity of PTE, effectively lowered blood glucose, improved the antioxidant capacity and reduced the inflammatory response. The NPs prepared with glucose sensitive material AAPBA provide a "switch" for insulin release in diabetic patients. PTE expands its application in the treatment of diabetes through NPs or other drug delivery media. In addition, plant extracts, similar to salidrome extract, ginseng extract, tea polyphenols, theanine and anthocyanins, play an important role in improving cardiovascular function, anti-cancer, prevention and treatment of diabetes and immune system. We predict that nano delivery system will provide new application prospects for the wide application of plant extracts in the future.

Abbreviations

PTE (pterostilbene); AAPBA (3-acrylamidophenyl boric acid)；NPs: nanoparticles; p(AAPBA-b-PTE): ploy (3-acrylamidophenyl boric acid-b-pterostilbene).

Declarations

Authors' contributions

XZ prepared and characterized the p(AAPBA-b-PTE) NPs, and analyzed the data and drafted the manuscript. AHS assisted with the functionalization of the nanocomposite. QM and YXY performed the in vitro and in vivo experiments. Junzi Wu and Pengyue Zhang designed the experiment and wrote the respective procedures and results related to it in the manuscript. All authors read and approved the final manuscript.

Author details

[a] Yunnan Provincial Key Laboratory of Molecular Biology for Sinomedicine, School of Basic Medical, Yunnan University of Chinese Medicine, Kunming, Yunnan 650500, P.R. China.

[b] College of Clinical Medical, Kunming Medical University, Kunming, Yunnan 650500, PR China.

[c] College of Basic Medicine, Kunming Medical University, Kunming, Yunnan 650500, PR China.

[d] Key Laboratory of acupuncture and tuina for treatment of encephalopathy, College of Acupuncture, Tuina and Rehabilitation, Yunnan University of Traditional Chinese Medicine, Kunming, 650500, China.

Acknowledgements

This investigation was supported by the grant from the Key Laboratory of Microcosmic Syndrome Differentiation, Education Department of Yunnan Project (20190720); Yunnan Province Natural Science Foundation of China (30172110104)Yunnan Province Applied Basic Research Project (2019FF002 (-055)).

Competing interests

The authors declare no competing financial interest.

Availability of data and materials

All data generated or analyzed during this study are included in this published article.

Ethics approval and consent to participate

All animal experiments were undertaken following robust ethical review and in accordance with the procedures authorized by the Committee for Experimental Animal Welfare and Ethics of Yunnan University of Traditional Chinese Medicine.

References

1. The Lancet. Diabetes: a dynamic disease. 2017 Jun 3;389(10085):2163.
2. Forbes JM, Cooper ME. Mechanisms of diabetic complications. *Physiol Rev.* 2013 Jan;93(1):137-88.
3. Valeri C, Pozzilli P, Leslie D. Glucose control in diabetes. *Diabetes Metab Res Rev.* 2004 Nov-Dec;20 Suppl 2:S1-8.
4. van der Schaft N, Schoufour JD, Nano J, Kiefte-de Jong JC, Muka T, Sijbrands EJG, Ikram MA, Franco OH, Voortman T. Dietary antioxidant capacity and risk of type 2 diabetes mellitus, prediabetes and insulin resistance: the Rotterdam Study. *Eur J Epidemiol.* 2019 Sep;34(9):853-861.
5. Zhong Y, Song B, He D, Xia Z, Wang P, Wu J, Li Y. Galactose-based polymer-containing phenylboronic acid as carriers for insulin delivery. 2020 Sep 25;31(39):395601.

6. Ma Q, Zhao X, Shi A, Wu J. Bioresponsive Functional Phenylboronic Acid-Based Delivery System as an Emerging Platform for Diabetic Therapy. *Int J Nanomedicine.* 2021 Jan 12;16:297-314.
7. Gunasekara RW, Zhao Y. A General Method for Selective Recognition of Monosaccharides and Oligosaccharides in Water. *J Am Chem Soc.* 2017 Jan 18;139(2):829-835.
8. Gunasekara RW, Zhao Y. A General Method for Selective Recognition of Monosaccharides and Oligosaccharides in Water. *J Am Chem Soc.* 2017 Jan 18;139(2):829-835.
9. Zhao L, Xiao C, Wang L, Gai G, Ding J. Glucose-sensitive polymer NPs for self-regulated drug delivery. *Chem Commun (Camb).* 2016 Jun 8;52(49):7633-52.
10. Ryu JH, Lee GJ, Shih YV, Kim TI, Varghese S. Phenylboronic Acid-polymers for Biomedical Applications. *Curr Med Chem.* 2019;26(37):6797-6816.
11. Matsumoto A Ikeda S Harada A Kataoka K. Glucose-responsive polymer bearing a novel phenylborate derivative as a glucose-sensing moiety operating at physiological pH conditions. 2003 Sep-Oct;4(5):1410-6.
12. Zheng C, Guo Q, Wu Z, Sun L, Zhang Z, Li C, Zhang X. Amphiphilic glycopolymer NPs as vehicles for nasal delivery of peptides and proteins. *Eur J Pharm Sci.* 2013 Jul 16;49(4):474-82.
13. Wu JZ, Yang Y, Li S, Shi A, Song B, Niu S, Chen W, Yao Z. Glucose-Sensitive Nanoparticles Based On Poly(3-Acrylamidophenylboronic Acid-Block-N-Vinylcaprolactam) For Insulin Delivery. *Int J Nanomedicine.* 2019 Oct 4;14:8059-8072.
14. Wu JZ, Bremner DH, Li HY, Niu SW, Li SD, Zhu LM. Phenylboronic acid-diol crosslinked 6-O-vinylazeloyl-d-galactose nanocarriers for insulin delivery. Mater Sci Eng C Mater Biol Appl. 2017 Jul 1;76:845-855.
15. Wu JZ, Williams GR, Li HY, Wang D, Wu H, Li SD, Zhu LM. Glucose- and temperature-sensitive nanoparticles for insulin delivery. *Int J Nanomedicine.* 2017 May 29;12:4037-4057.
16. Elsaesser A, Howard CV. Toxicology of NPs. *Adv Drug Deliv Rev.* 2012 Feb;64(2):129-37.
17. Xie B, Xu Z, Hu L, Chen G, Wei R, Yang G, Li B, Chang G, Sun X, Wu H, Zhang Y, Dai B, Tao Y, Shi J, Zhu W. PTE Inhibits Human Multiple Myeloma Cells via ERK1/2 and JNK Pathway In Vitro and In Vivo. *Int J Mol Sci.* 2016 Nov 17;17(11):1927.
18. Tsai HY, Ho CT, Chen YK. Biological actions and molecular effects of resveratrol, PTE, and 3'-hydroxyPTE. *J Food Drug Anal.* 2017 Jan;25(1):134-147.
19. Kosuru R, Rai U, Prakash S, Singh A, Singh S. Promising therapeutic potential of PTE and its mechanistic insight based on preclinical evidence. *Eur J Pharmacol.* 2016 Oct 15;789:229-243.
20. McCormack D, McFadden D. PTE and cancer: current review. *J Surg Res.* 2012 Apr;173(2):e53-61.
21. Nagao K, Jinnouchi T, Kai S, Yanagita T. PTE, a dimethylated analog of resveratrol, promotes energy metabolism in obese rats. *J Nutr Biochem.* 2017 May;43:151-155.
22. Liu H, Wu X, Luo J. PTE Attenuates Astrocytic Inflammation and Neuronal Oxidative Injury After Ischemia-Reperfusion by Inhibiting NF-κB Phosphorylation. *Front Immunol.* 2019 Oct 17;10:2408.

23. Tastekin B, Pelit A, Polat S, Tuli A, Sencar L, Alparslan MM, Daglioglu YK. Therapeutic Potential of PTE and Resveratrol on Biomechanic, Biochemical, and Histological Parameters in Streptozotocin-Induced Diabetic Rats. *Evid Based Complement Alternat Med.* 2018 May 16;2018:9012352.
24. Kosuru R, Singh S. PTE ameliorates insulin sensitivity, glycemic control and oxidative stress in fructose-fed diabetic rats. *Life Sci.* 2017 Aug 1;182:112-121.
25. Remsberg CM, Yáñez JA, Ohgami Y, Vega-Villa KR, Rimando AM, Davies NM. Pharmacometrics of pterostilbene: preclinical pharmacokinetics and metabolism, anticancer, antiinflammatory, antioxidant and analgesic activity. *Phytother Res.* 2008 Feb;22(2):169-79.
26. Zeng Q, Lian W, Wang G, Qiu M, Lin L, Zeng R. Pterostilbene induces Nrf2/HO-1 and potentially regulates NF-κB and JNK-Akt/mTOR signaling in ischemic brain injury in neonatal rats. 3 2020 May;10(5):192.
27. Perecko T, Drabikova K, Rackova L, Ciz M, Podborska M, Lojek A, Harmatha J, Smidrkal J, Nosal R, Jancinova V. Molecular targets of the natural antioxidant pterostilbene: effect on protein kinase C, caspase-3 and apoptosis in human neutrophils in vitro. *Neuro Endocrinol Lett.* 2010;31 Suppl 2:84-90.
28. Lin HS, Yue BD, Ho PC. Determination of PTE in rat plasma by a simple HPLC-UV method and its application in pre-clinical pharmacokinetic study. *Biomed Chromatogr.* 2009 Dec;23(12):1308-15.
29. Goyal SN, Reddy NM, Patil KR, Nakhate KT, Ojha S, Patil CR, Agrawal YO. Challenges and issues with streptozotocin-induced diabetes - A clinically relevant animal model to understand the diabetes pathogenesis and evaluate therapeutics. *Chem Biol Interact.* 2016 Jan 25;244:49-63.
30. Heydemann A. An Overview of Murine High Fat Diet as a Model for Type 2 Diabetes Mellitus. *J Diabetes Res.* 2016;2016:2902351.
31. Zhang X, Wang Y, Zheng C, Li C. Phenylboronic acid-functionalized glycopolymeric nanoparticles for biomacromolecules delivery across nasal respiratory. *Eur J Pharm Biopharm.* 2012 Sep;82(1):76-84.
32. Liu S, Ono RJ, Yang C, Gao S, Ming Tan JY, Hedrick JL, Yang YY. Dual pH-Responsive Shell-Cleavable Polycarbonate Micellar Nanoparticles for in Vivo Anticancer Drug Delivery. ACS *Appl Mater Interfaces.* 2018 Jun 13;10(23):19355-19364.
33. Moghadamtousi SZ, Kadir HA, Hassandarvish P, Tajik H, Abubakar S, Zandi K. A review on antibacterial, antiviral, and antifungal activity of curcumin. *Biomed Res Int.* 2014;2014:186864.
34. Yavarpour-Bali H, Ghasemi-Kasman M, Pirzadeh M. Curcumin-loaded NPs: a novel therapeutic strategy in treatment of central nervous system disorders. *Int J Nanomedicine.* 2019 Jun 17;14:4449-4460.
35. Moballegh Nasery M, Abadi B, Poormoghadam D, Zarrabi A, Keyhanvar P, Khanbabaei H, Ashrafizadeh M, Mohammadinejad R, Tavakol S, Sethi G. Curcumin Delivery Mediated by Bio-Based NPs: A Review. 2020 Feb 6;25(3):689.
36. Meng R, Wu Z, Xie QT, Cheng JS, Zhang B. Preparation and characterization of zein/carboxymethyl dextrin NPs to encapsulate curcumin: Physicochemical stability, antioxidant activity and controlled release properties. *Food Chem.* 2021 Mar 15;340:127893.

37. Li X, Pennington J, Stobaugh JF, Schöneich C. Synthesis of sulfonamide- and sulfonyl-phenylboronic acid-modified silica phases for boronate affinity chromatography at physiological pH. *Anal Biochem.* 2008 Jan 15;372(2):227-36.
38. Zhao L, Xiao C, Wang L, Gai G, Ding J. Glucose-sensitive polymer NPs for self-regulated drug delivery. *Chem Commun (Camb).* 2016 Jun 8;52(49):7633-52.
39. Guo Q, Wu Z, Zhang X, Sun L, Li C. Phenylboronate-diol crosslinked glycopolymeric nanocarriers for insulin delivery at physiological pH. *Soft Matter.* 2014 Feb 14;10(6):911-20.
40. Ayubi M, Karimi M, Abdpour S, Rostamizadeh K, Parsa M, Zamani M, Saedi A. Magnetic NPs decorated with PEGylated curcumin as dual targeted drug delivery: Synthesis, toxicity and biocompatibility study. *Mater Sci Eng C Mater Biol Appl.* 2019 Nov;104:109810.
41. Li M, Zou P, Tyner K, Lee S. Physiologically Based Pharmacokinetic (PBPK) Modeling of Pharmaceutical NPs. *AAPS J.* 2017 Jan;19(1):26-42.
42. Zhang X, Lü S, Gao C, Chen C, Zhang X, Liu M. Highly stable and degradable multifunctional microgel for self-regulated insulin delivery under physiological conditions. 2013 Jul 21;5(14):6498-506.
43. Mumuni MA, Kenechukwu FC, Ofokansi KC, Attama AA, Díaz DD. Insulin-loaded mucoadhesive NPs based on mucin-chitosan complexes for oral delivery and diabetes treatment. *Carbohydr Polym.* 2020 Feb 1;229:115506.
44. Chen T, Liu W, Xiong S, Li D, Fang S, Wu Z, Wang Q, Chen X. NPs Mediating the Sustained Puerarin Release Facilitate Improved Brain Delivery to Treat Parkinson's Disease. *ACS Appl Mater Interfaces.* 2019 Dec 4;11(48):45276-45289.
45. Wang P, Sang S. Metabolism and pharmacokinetics of resveratrol and pterostilbene. 2018 Jan;44(1):16-25.
46. Sanna V, Roggio AM, Siliani S, Piccinini M, Marceddu S, Mariani A, Sechi M. Development of novel cationic chitosan-and anionic alginate-coated poly(D,L-lactide-co-glycolide) NPs for controlled release and light protection of resveratrol. *Int J Nanomedicine.* 2012;7:5501-16.
47. Zielińska A, Carreiró F, Oliveira AM, Neves A, Pires B, Venkatesh DN, Durazzo A, Lucarini M, Eder P, Silva AM, Santini A, Souto EB. Polymeric NPs: Production, Characterization, Toxicology and Ecotoxicology. 2020 Aug 15;25(16):3731.
48. Zhou J, Zhang J, Gao G, Wang H, He X, Chen T, Ke L, Rao P, Wang Q. Boiling Licorice Produces Self-Assembled Protein NPs: A Novel Source of Bioactive Nanomaterials. *J Agric Food Chem.* 2019 Aug 21;67(33):9354-9361.
49. Feng L, Yang X, Shi Y, Liang S, Zhao T, Duan J, Sun Z. Co-exposure subacute toxicity of silica NPs and lead acetate on cardiovascular system. *Int J Nanomedicine.* 2018 Nov 21;13:7819-7834.
50. Suksangrat T, Phannasil P, Jitrapakdee S. miRNA Regulation of Glucose and Lipid Metabolism in Relation to Diabetes and Non-alcoholic Fatty Liver Disease. *Adv Exp Med Biol.* 2019;1134:129-148.
51. Mohammadpour R, Dobrovolskaia MA, Cheney DL, Greish KF, Ghandehari H. Subchronic and chronic toxicity evaluation of inorganic NPs for delivery applications. *Adv Drug Deliv Rev.* 2019 Apr;144:112-

132.

52. De Jong WH, Borm PJ. Drug delivery and NPs:applications and hazards. *Int J Nanomedicine.* 2008;3(2):133-49.
53. Hu Q, Luo Y. Recent advances of polysaccharide-based nanoparticles for oral insulin delivery. *Int J Biol Macromol.* 2018 Dec;120(Pt A):775-782.
54. Taili Shao T, Yuan P, Zhu L, Xu H, Li X, He S, Li P, Wang G, Chen K. Carbon NPs Inhibit A-Glucosidase Activity and Induce a Hypoglycemic Effect in Diabetic Mice. 2019 Sep 6;24(18):3257.
55. Goycheva P, Nikolova G, Ivanova M, Kundurdzhiev T, Gadjeva V. Predictive value of some pro-oxidants in type 2 diabetes mellitus with vascular complications. *Biosci Trends.* 2019 May 12;13(2):168-175.
56. King GL. The role of inflammatory cytokines in diabetes and its complications. *J Periodontol.* 2008 Aug;79(8 Suppl):1527-34.
57. Yousuf O, Mohanty BD, Martin SS, Joshi PH, Blaha MJ, Nasir K, Blumenthal RS, Budoff MJ. High-sensitivity C-reactive protein and cardiovascular disease: a resolute belief or an elusive link? *J Am Coll Cardiol.* 2013 Jul 30;62(5):397-408.
58. Zhang X, Lü S, Gao C, Chen C, Zhang X, Liu M. Highly stable and degradable multifunctional microgel for self-regulated insulin delivery under physiological conditions. 2013 Jul 21;5(14):6498-506.

Tables

Table 1 Study the polymerization reaction of different ratios (AAPBA, PTE) and AIBN.

Samples	p(AAPBA)	PTE	AIBN	yield
p(AAPBA-b-PTE)1	1000	500mg	1.5 mg	79.4%
p(AAPBA-b-PTE)2	1000	100mg	1.2 mg	80.2%
p(AAPBA-b-PTE)3	1000	50mg	1.1 mg	77.1%

The yield was calculated using the final collected polymer amount/the input material amount.

Table 2 Insulin LC and EE of p(AAPBA-b-PTE□NPs

Samples	Insulin concentration(mg/mL)	EE(%)	LC(%)
p(AAPBA-b-PTE)1	1.00	55.1±5.4	13.3±1.6
p(AAPBA-b-PTE)2	1.00	56.7±6.1	13.8±1.4
p(AAPBA-b-PTE)3	1.00	58.3±5.1	14.5±1.2

Notes: Data are presented as mean ± standard deviation.

Abbreviations: EE, encapsulation efficiency; LC, drug loading.

Table 3 Effect of administration by injection of the NPs on the biochemical parameters of rats after 14 d (n = 5, mean ± SD).

Index/Groups	Normal	P(AAPBA-b-PTE)2		
		10 mg/kg/d	50mg/kg/d	100mg/kg/d
RBC($\times10^6\mu l^{-1}$)	10.42±0.45	10.35±0.68	10.38±0.46	10.51±0.34
MCV (fL)	41.56±1.06	40.89±0.98	41.23±1.14	41.68±1.14
RDW(%CV)	17.95±2.54	18.01±2.34	18.12±2.18	18.24±2.21
HCT (vol.%)	43.03±2.01	42.80±1.86	42.95±2.04	43.01±1.95
MCH (pg)	13.85±0.86	13.80±0.78	13.92±0.65	13.95±0.62
MCHC (g/L)	33.40±1.53	33.80±1.68	33.50±1.48	33.62±1.54
WBC ($\times10^3\mu l^{-1}$)	7.95±1.25	7.80±1.15	8.02±0.95	7.90±1.20
NE (%)	18.22±2.57	18.24±2.38	18.19±2.26	18.12±2.12
EO (%)	2.72±1.18	2.70±1.22	2.74±1.12	2.70±1.20
BA (%)	1.80±0.64	1.79±0.58	1.81±0.70	1.78±0.54
LY (%)	74.01±3.09	74.31±2.85	73.69±2.92	74.19±2.68
MO (%)	2.38±0.58	2.40±0.37	2.35±0.65	2.34±0.50
PLT（$10^3/mm^3$）	768.20±150.80	770.35±145.54	776.25±153.40	765.38±148.26
MPV (fL)	6.01±1.78	5.98±1.69	6.04±1.70	6.03±0.26

Figures

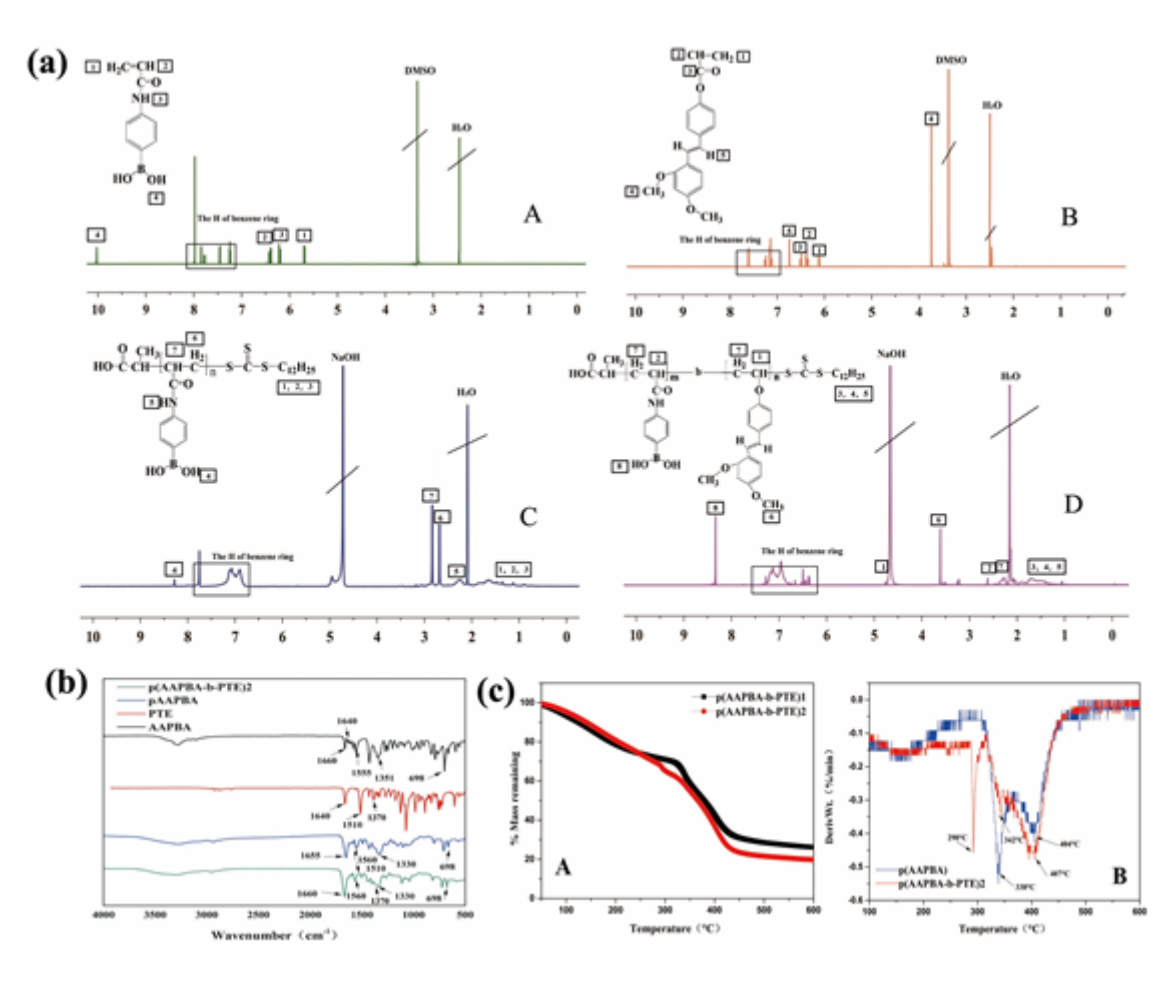

Figure 1

(a) 1H-NMR spectra results of AAPBA(A); PTE(B); p(AAPBA)(C); p(AAPBA-b-PTE)(D). (b) FT-IR spectra results. (c) Thermal analysis of the polymers: DTG(A) and TG(B).

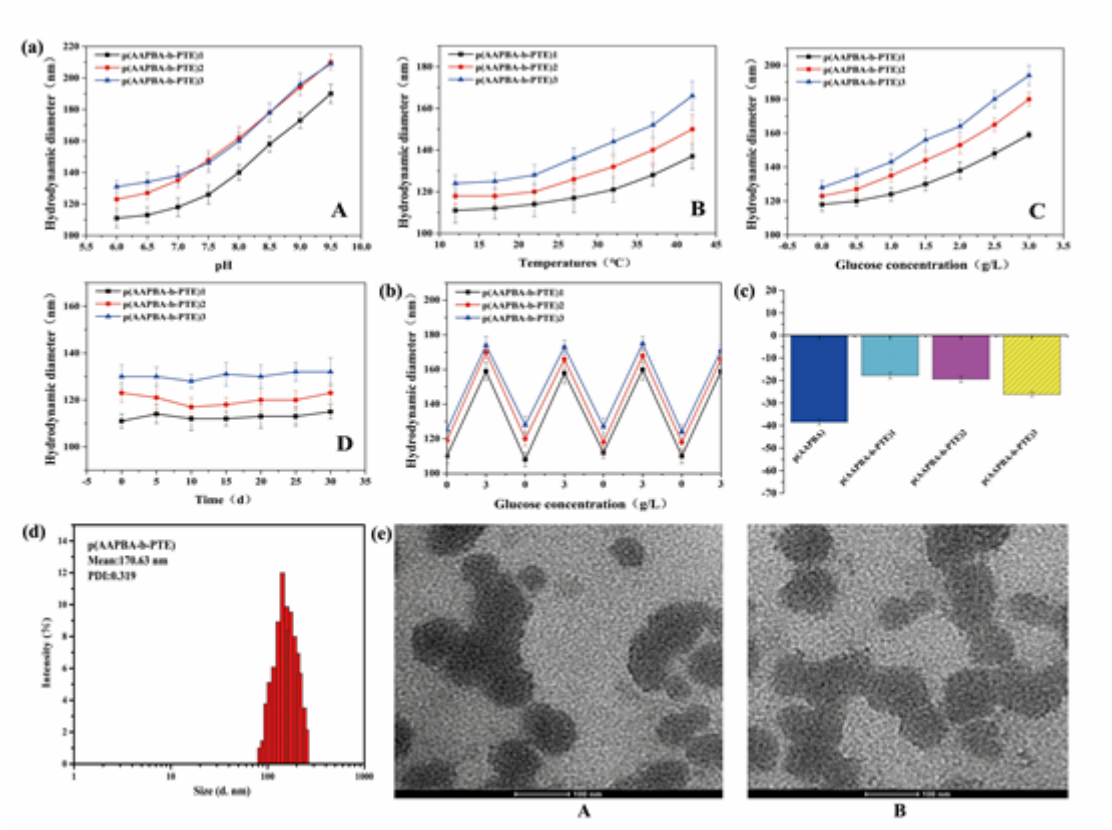

Figure 2

(a)The change of different hydrodynamic diameters is as follows: PH(A); temperature (B); glucose concentration(C); (D) is the p(AAPBA-b-PTE) of stability in pH 7.4 PBS. (b) Results of glucose sensitive elasticity of NPs. (c) The zeta potentials of the p(AAPBA-b-PTE). (d) The Particle size and PDI of the p(AAPBA-b-PTE). (e)TEM change diagram of p(AAPBA-b-PTE)2 NPs:(A) in PBS solution (B) in 3 mg/mL glucose concentration 72 hours.

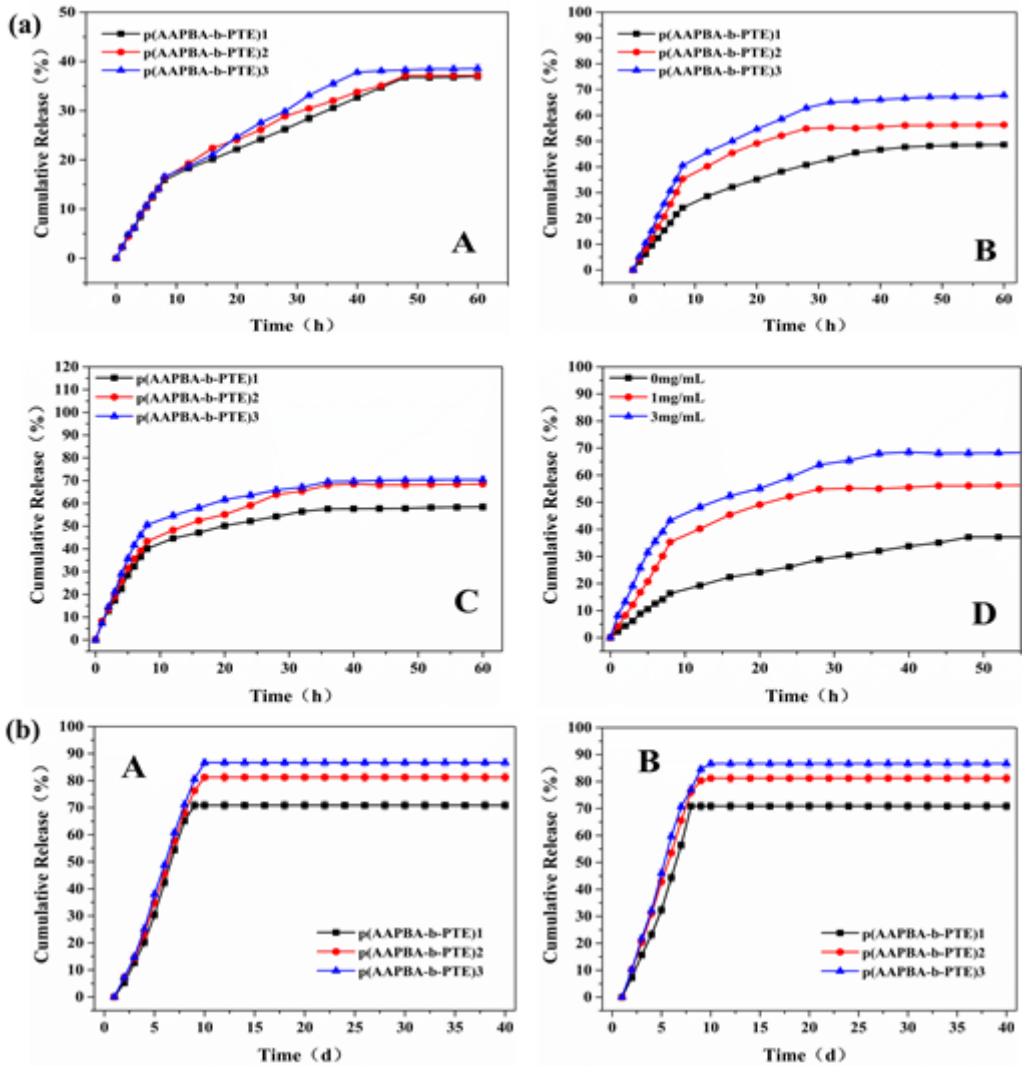

Figure 3

(a) The cumulative insulin release of p(AAPBA-b-PTE) NPs in vitro with glucose concentration of 0mg/ml (A), 1mg/ml (B) and 3mg/ml (C). (D) is the cumulative insulin release of P(AAPBA-b-PTE)2. (b) The cumulative PTE release of p(AAPBA-b-PTE) NPs in vitro with glucose concentration of 0 mg/ml (A) and 3 mg/ml (B).

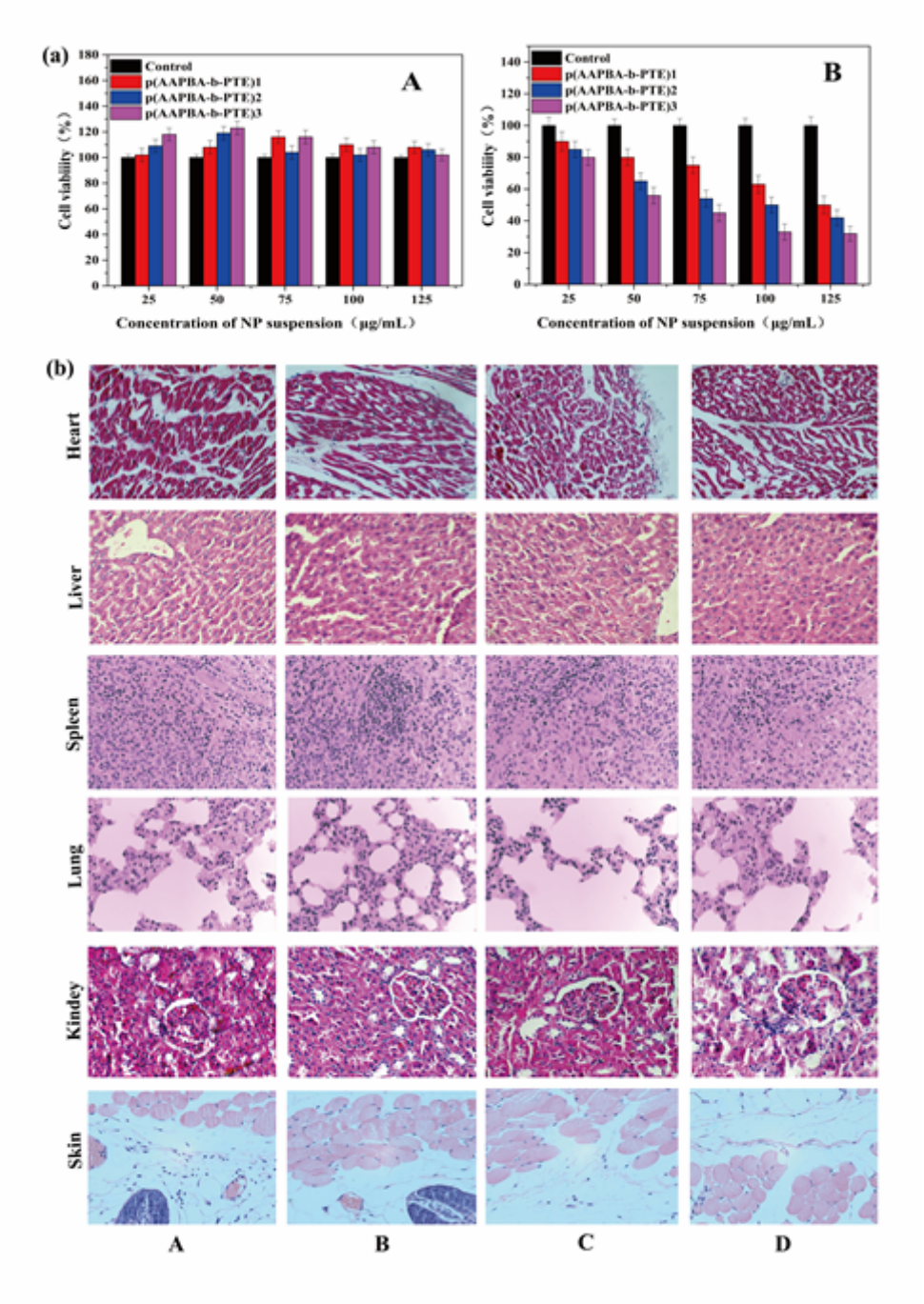

Figure 4

(a) Cell viability as a function of the concentration of p(AAPBA-b-PTE) NPs by the MTT assay at 37 °C after the incubation for 24 h. Each value represents the mean ± SD (n = 5) (b) HE staining representative images of heart, liver, spleen, lung, kidney and skin in control group(A), diabetic group(B), p(AAPBA-b-PTE)2 group(C), insulin injection treated group(D).

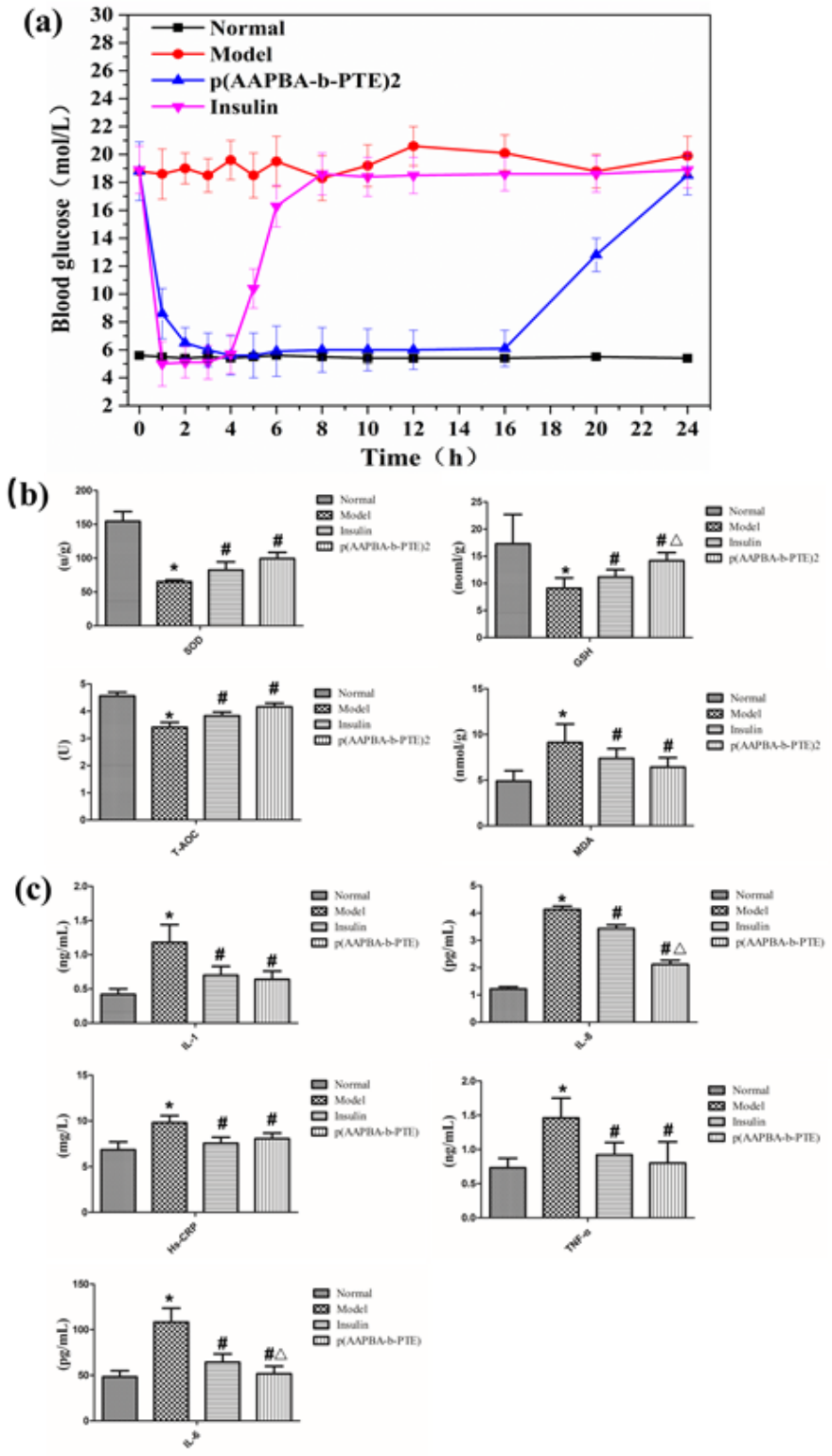

Figure 5

(a) Blood glucose concentration after injection over 24h. (b) Oxidation index and microinflammatory index of mice in each group after 2 weeks.

Supplementary Files

This is a list of supplementary files associated with this preprint. Click to download.

- Scheme01.png
- Scheme02.png
- AdditionalInformation.docx